Crustal structure of the Chicxulub Impact crater imaged with magnetotelluric exploration

Martyn Unsworth
University of Alberta, Edmonton, Canada

Oscar Campos Enriquez
Instituto de Geofisica, Universidad Nacional Autónoma de México (UNAM), México D.F., México

Salvador Belmonte
CIIDIR-Oaxaca, Instituto Politecnico Nacional, Oaxaca, México

Jorge Arzate
UNAM-UNICIT, Universidad Nacional Autónoma de México, Quéretaro, México

Paul Bedrosian
Department of Earth and Space Sciences, University of Washington, Seattle, USA

Received 26 February 2002; revised 29 April 2002; accepted 2 May 2002; published 24 August 2002.

[1] The electrical resistivity structure of the Chicxulub Impact crater has been imaged using broadband magnetotelluric exploration. A 1–2 km thick sequence of conductive Tertiary sedimentary rocks was imaged within the crater. The shallow resistivity of this layer increases across the cenote ring. This is primarily due to a decrease in porosity, although the groundwater composition may have some effect. While this layer reduces the sensitivity of MT, several features can be discerned beneath it. In the center of the crater the structural high is imaged as a region of high resistivity. In the outer part of the crater, lower resistivities in the upper crust may be due to mineralization or hydrothermal alteration. *INDEX TERMS:* 5420 Planetology: Solid Surface Planets: Impact phenomena (includes cratering); 0925 Exploration Geophysics: Magnetic and electrical methods

1. Introduction

[2] The Chicxulub Impact Crater in Mexico has been conclusively linked with the impact of an extraterrestrial body at the end of the Cretaceous period [*Hildebrand et al.*, 199l]. Gravity and magnetic field data were initially used to map the structure and revealed a characteristic pattern of multiple concentric anomalies. These data indicate that the diameter of the structure is around 180 km [*Hildebrand et al.*, 1995], but larger diameters have been reported [*Espindola et al.*, 1995; *Sharpton et al.*, 1993]. The primary surface expression of the crater is a ring of sinkholes (cenotes) that are coincident with the crater rim [Figure 1; *Perry et al.*, 1995]. Seismic reflection surveys over the offshore portion of the crater showed that the radius of the collapsed disruption cavity is around 45 km [*Camargo and Suarez*, 1994; *Morgan et al.*, 1997]. Tying the offshore seismic reflection data to the gravity data allows the shallow structure to be mapped onshore [*Hildebrand et al.*, 1998]. Seismic refraction data imaged the Tertiary crater fill and the central uplift [*Christeson et al.*, 2001].

[3] The magnetotelluric (MT) method provides images of crustal resistivity using natural, low frequency electromagnetic waves. MT data were first collected at Chicxulub by UNAM [*Campos et al.*, 1997] and detected a 1–2 km thick layer of low resistivity crater fill. This layer decreases the sensitivity of MT data to structure below. In this paper we present the results of a more extensive MT study that was undertaken to evaluate the potential of MT for exploration of the crustal structure of the Chicxulub Impact Crater.

2. Data Collection and Processing

[4] Broadband magnetotelluric (MT) data were collected in 2001 at 40 stations on two radial profiles that extended from the center of the crater to a radial distance of approximately 110 km (Figure 1). These profiles were located in the southeast portion of the crater where cultural noise was relatively low. Line 1 was coincident with the onshore seismic profile Chicx-F of *Morgan et al.* [1997]. MT data were recorded in remote reference mode to permit noise removal. The data were processed with the algorithm of *Egbert* [1997] and gave estimates of apparent resistivity and phase in the frequency band 100–0.0003 Hz. Tensor decomposition was used to determine the dimensionality of the data [*McNeice and Jones*, 2001]. The MT data were undistorted and two-dimensional, with best-fitting strike directions of N45°E and N70°E for Lines 1 and 2 respectively (Figure 1). These directions are orthogonal to the profiles and show that the geo-electric strike is dominated by structural changes in the radial direction. MT data from a typical site (cxb005) on Line 1 are shown in Figure 2 in a co-ordinate system that is parallel to Line 1. Thus the so-called transverse magnetic (TM) mode data were computed from electric currents flowing along the radial profile, while the transverse electric (TE) mode data were computed from electric currents flowing orthogonal to the profile. At 10 Hz the apparent resistivity is ~3 ohm-m. As the frequency decreases the signals

0094-8276/02/2002GL014998$05.00

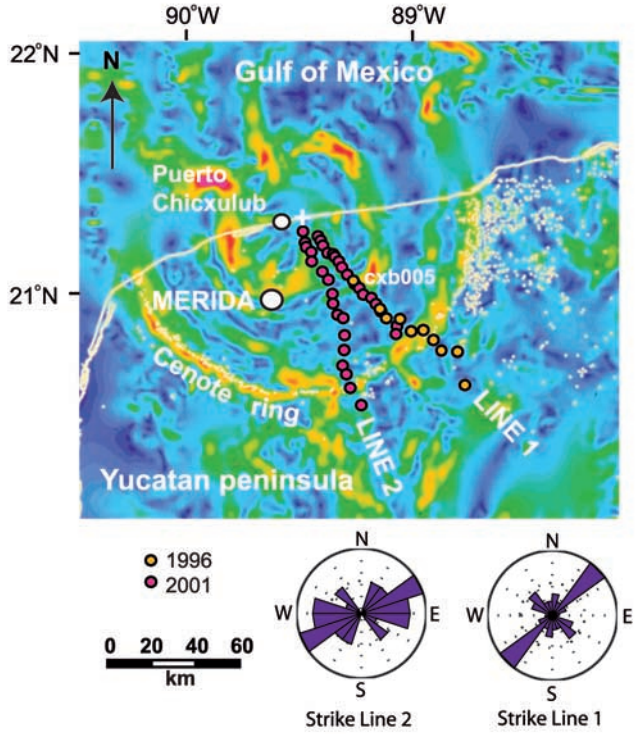

Figure 1. Location of MT profiles superimposed on the horizontal gradient of the Bouguer gravity anomaly [*Hildebrand et al.*, 1995]. The histograms show the geoelectric strike direction for the 10−0.001 Hz frequency band at each site. The white dots are cenotes (sinkholes), and the cross the center of the impact structure.

penetrate the conductive sedimentary rocks in the Tertiary basin and the apparent resistivity decreases. Below 0.3 Hz the apparent resistivity rises as signals sample the resistive Cretaceous sedimentary and crystalline basement rocks. The same basic shape of apparent resistivity curve was observed at most of the MT measurement locations on Lines 1 and 2. However, subtle variations are observed on both MT profiles as a function of radial distance. These changes are illustrated

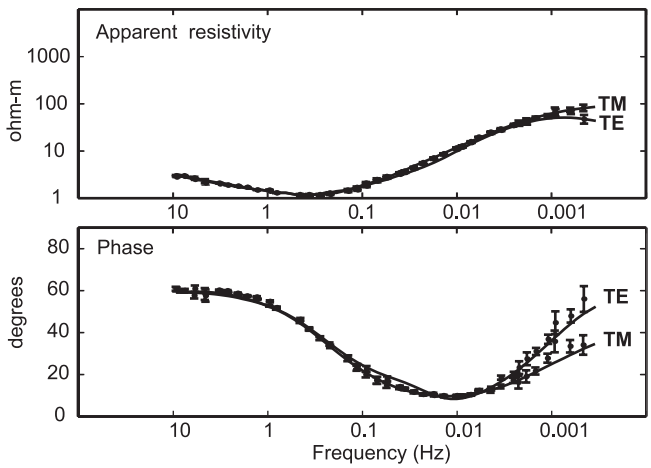

Figure 2. Apparent resistivity measured at station cxb005 on Line 1. The continuous line shows the responses of the resistivity model in Figure 4.

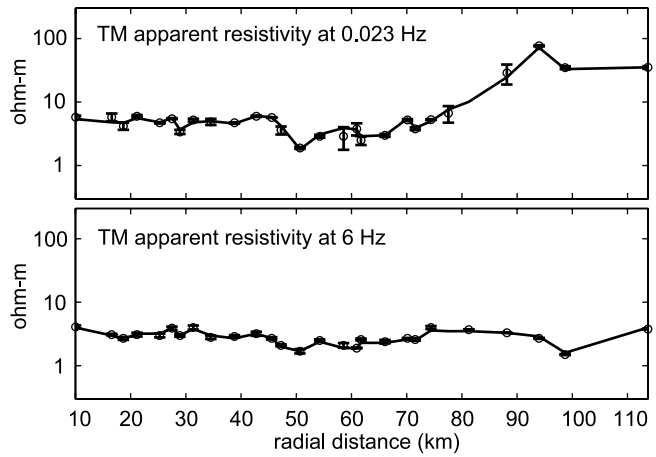

Figure 3. TM apparent resistivity as a function of radial distance on Line 1 for frequencies of 6 Hz and 0.023 Hz. The continuous line shows the responses of the resistivity model in Figure 4.

in Figure 3 where apparent resistivity is plotted as a function of radial distance. At 6 Hz the MT signals are sample shallow structure and the apparent resistivity shows little variation with radial distance. At lower frequencies (period 44 s) a characteristic variation can be seen. In the center of the crater the apparent resistivity is ∼10 ohm-m. At a radial distance of ∼45 km the apparent resistivity falls by half an order of magnitude, and then at 75 km it begins a significant increase. This pattern is observed over a wide frequency band, in both the TE and TM modes and on both Lines 1 and 2.

[5] To convert the measured MT data into a resistivity model of the subsurface, the inversion algorithm of *Rodi and Mackie* [2001] was used. The use of a two-dimensional inversion is justified from the tensor decomposition described above, and also by the similarity of the models derived for Lines 1 and 2 (Figure 4). These models were computed by inverting the TM mode data and fit the data on Lines 1 and 2 with normalized misfits of 1.00 and 1.20 respectively. Similar models were obtained by inverting the TE data. The inversion algorithm seeks the smoothest resistivity model that is consistent with fitting the data. Thus while models with more structure could be found, they are not required by the data. The MT data were inverted using a wide range of parameters and starting models, and the same basic model was recovered in each case. This process also included the estimation of static shift coefficients, which were shown to have a negligible effect on the final resistivity model. The fit at site cxb005 is shown in Figure 2, and the fit as a function of radial distance is shown in Figure 3. In both models the upper 100−200 m of the model is moderately resistive (hard to see in Figure 4) and is underlain by a 1−2 km thick conductive layer. As expected, this conductor has the effect of diminishing resolution of crustal structure below, but some long wavelength features can be discerned. Beyond a radius of 70 km relatively resistive rocks are imaged below a depth of ∼5 km. From 40 to 70 km radius, the upper crust below has an intermediate resistivity (∼100 ohm-m). From 40 km to the center of the crater, the upper crust is again resistive. MT determines the conductance of a layer (the product of conductivity and thickness), so a thinner, but more conductive, layer would also fit the

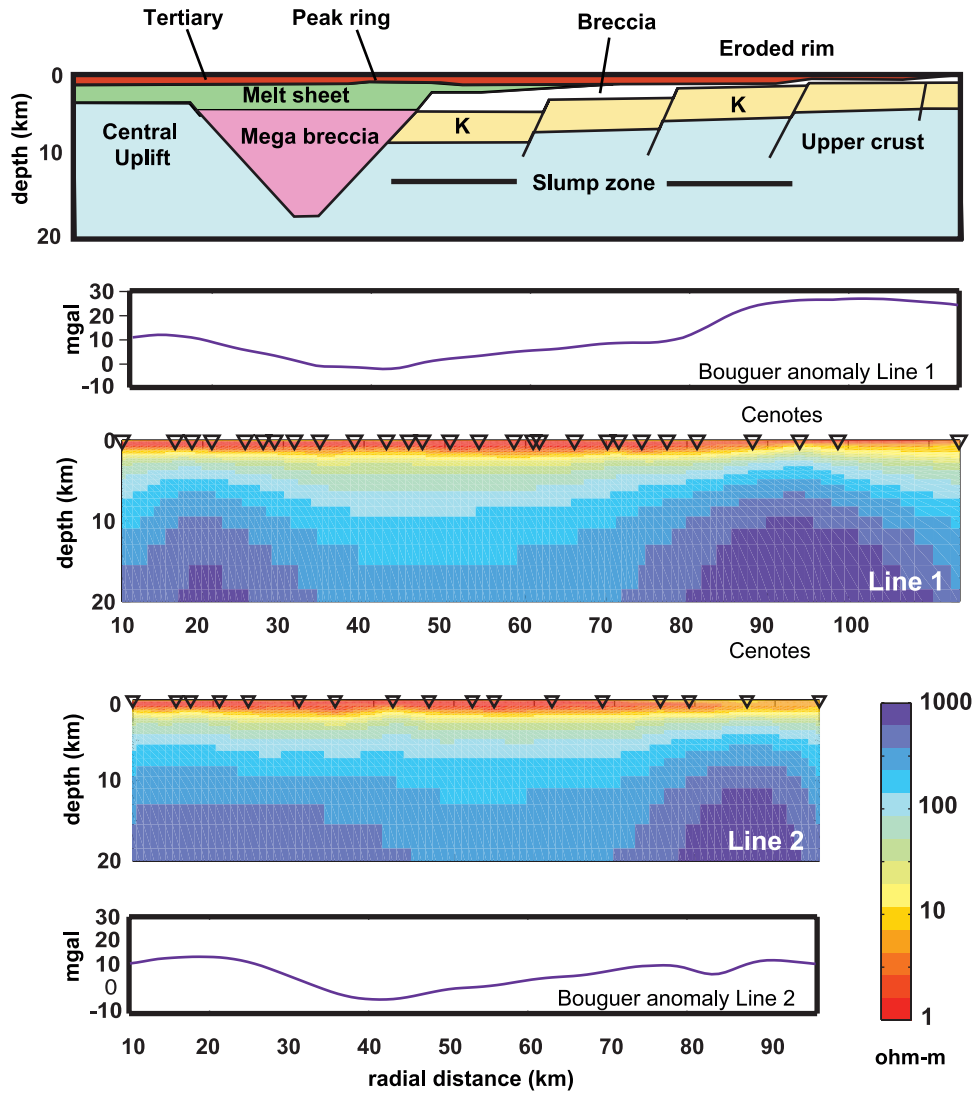

Figure 4. Two-dimensional resistivity models derived by inverting the MT data for Lines 1 and 2. The Bouguer anomaly for each profile is also shown [*Hildebrand et al.*, 1995]. The line drawing is adapted from *Hildebrand et al.* [1998].

MT data. Thus the thickness of the low resistivity layer in the upper crust (beneath the Tertiary section) cannot be uniquely determined. It should also be noted that while the MT response of this feature is relatively weak, its detection is permitted by the very uniform electrical structure in the upper 2 km. Some edge effects may be present in the resistivity models shown in Figure 4, but these are limited to the end stations on each profile.

3. Interpretation

[6] The shallow resistive zone on both models in the upper 200 m is primarily due to resistive carbonate rocks saturated with fresh groundwater. Beneath the shallow freshwater aquifer the groundwater in the Yucatan is uniformly saline on both sides of the cenote ring [*Marin*, 1990], and this saline groundwater produces the low resistivity observed in the upper 1–2 km. The underlying conductive layer is remarkably uniform across the crater, and has a resistivity close to 1 ohm-m. The thickness of these units derived from the MT data (1–2 km) agrees with both seismic data and well logs [*Christeson et al.*, 2001; *Ward et al.*, 1995]. Within 40 km of the coast the saline fluids are derived from a mixture of seawater and freshwater [*Perry et al.*, 1995]. Further inland the high salinity may be Tdue to the dissolution of evaporites [*Perry et al.*, 1995], yet the conductance of the layer remains relatively constant from the coast to the cenote ring. Outside the cenote ring a shallow conductive layer is also present, but its conductance is an order of magnitude less than within the ring (Figure 4). The cenote ring is associated with a shallow valley in the water table and acts as a high permeability channel that allows groundwater to flow to the coast [*Marin*, 1990; *Perry et al.*, 1995]. Thus the change in electrical properties across the cenote ring may not be solely due to the composition of the groundwater, and may reflect a higher porosity in the sedimentary rocks within the cenote ring. The pre-impact Yucatan geology was characterized by 2–3 km of Cretaceous carbonates and evaporites overlying crystalline basement. These sedimentary rocks are still present outside the crater and are generally shallow water, coarse-grained carbonates with a low porosity. In contrast the Tertiary

rocks deposited within the crater are pelitic and have a higher porosity [A. Hildebrand, personal communication, 2002; *Ward et al.*, 1995]. The presence of resistive upper crustal rocks outside the cenote ring is due to undisturbed Cretaceous carbonates and crystalline basement beneath the zone of saline groundwater.

[7] In the outer part of the crater (40–80 km radius) the upper crust is an order of magnitude more conductive than the upper crust outside the cenote ring. Seismic, gravity and magnetic exploration has shown that this zone is comprised of breccia, melt-sheet and slumped blocks [Figure 4; *Hildebrand et al.*, 1998; *Camargo and Suarez*, 1994; *Morgan et al.*, 1997]. Why should the upper crustal rocks in this area have a relatively low resistivity? Interconnected fluids, such as groundwater, are often invoked to explain low resistivities in the shallow crust [*Palacky*, 1991]. This scenario requires that the fluids be interconnected over distances comparable to the scale of the feature. While this may be possible at Chicxulub, could a network of interconnected fractures could have remained open for 65 million years? An alternative explanation for these low resistivities could be the presence of mineralization or hydrothermal alteration [*Palacky*, 1991]. While extensive mineralization may be present at Chicxulub, it is more likely that the widespread low resistivities were produced by hydrothermal alteration that would have occurred as the melt sheet and breccias cooled. The alteration is found throughout the breccia and slumped blocks since fracturing would have created the necessary pathways for hydrothermal circulation. *Hildebrand and Pilkington* [2000] suggested that some magnetic field anomalies at Chicxulub are due to zones of hydrothermal alteration that underlie discrete mineral deposits. Regrettably, the lack of resolution due to the overlying conductive basin prevents individual mineral deposits being distinguished from a more diffusive zone of hydrothermal alteration using the MT data.

[8] The region of upper crustal low resistivity terminates at a radial distance of around 30 km. The high resistivity upper crust within this distance is an expression of the central structural uplift. A good correlation can be observed between the Bouguer anomaly and the extent of high resistivity in the center of the crater, as expected since the uplifted basement rocks have both high density and high electrical resistivity. The central uplift position is confirmed by the seismic studies [*Christeson et al.*, 2001].

4. Conclusions

[9] The magnetotelluric data have imaged the electrical resistivity structure of the Chicxulub Impact crater. The best resolved feature is the Tertiary crater fill, which shows a major change across the cenote ring in the upper 1–2 km. Resolution in the upper crust beneath the Tertiary fill is reduced by the presence of the conductive basin. Nevertheless, the structural high and a zone of low resistivity basement can be discerned in the outer part of the basin and is probably the result of hydrothermal alteration and mineralization.

[10] **Acknowledgments.** Funding from NSF (grant EAR9908851) and IPGH (grant 01–62) is gratefully acknowledged. The MT instruments were provided through the NSF funded EMSOC facility. Steve Park is thanked for his efforts preparing and shipping the instruments. This study was made possible by enthusiastic field assistance from Michael Lazorek, Ulli Zimmer, Ulysses Nuñez, David Rivera and Miguel Angel Alatorre. We acknowledge many discussions with Alan Hildebrand and Jaime Urrutia Fucugauchi. Reviews by Alan Hildebrand and an anonymous reviewer improved this paper. Assistance from Yucatan landowners was essential to the success of this study. Support from the local authorities was invaluable in obtaining permission from the landowners.

References

Camargo Zanoguera, A., and G. Suarez Reynoso, Evidencia sismica del crater de impacto de Chicxulub: *Boletin de la Asociacion Mexicana de Geofisicos de Exploracion*, *34*, 1–28, 1994.

Campos, J. O., J. A. Arzate, J. Urrutia-Fucugauchi, and O. Delgado-Rodriguez, The subsurface structure of the Chicxulub crater (Yucatan, Mexico): Preliminary results of a magnetotelluric study, *The Leading Edge*, 1774–1777, 1997.

Christeson, G. L., Y. Nakamura, R. Buffler, J. Morgan, and M. Warner, Deep crustal structure of the Chicxulub impact crater, *J. Geophys. Res.*, *106*, 21,751–21,769, 2001.

Egbert, G. D., Robust multiple-station magnetotelluric data processing, *Geophys. J. Int.*, *130*, 475–496, 1997.

Espindola, J. M., M. Mena, M. dela Fuente, and J. O. Campos-Enriquez, Chicxulub, A model of the Chicxulub structure based on its gravity and magnetic signature, *Physics of the Earth and Planetary Interiors*, *93*, 271–278, 1995.

Hildebrand, A. R., and M. Pilkington, Crater-floor exhalative (Crafex) sulfide deposits at the Chicxulub crater, Yucatan, Mexico: Abstract, GeoCanada, Calgary, 2000.

Hildebrand, A. R., G. T. Penfield, D. A. Kring, M. Pilkington, A. Camargo, S. B. Jacobsen, and W. V. Boynton, Chicxulub crater: A possible Cretaceous-Tertiary boundary impact crater on the Yucatan Peninsula, Mexico, *Geology*, *19*, 687–871, 1991.

Hildebrand, A. R., M. Pilkington, M. Connors, C. Ortiz-Aleman, and R. E. Chavez, Size and structure of the Chicxulub Impact crater on the Yucatan Peninsula, Mexico, *Nature*, *376*, 415–417, 1995.

Hildebrand, A. R., M. Pilkington, C. Ortiz-Aleman, R. E. Chavez, J. Urrutia Fucugauchi, M. Connors, E. Graniel Castro, A. Camara Zi, J. A. Halpenny, and D. Niehaus, Mapping Chicxulub crater structure with gravity and seismic reflection data, in *Meteorites: Flux with Time and Impact effects*, edited by M. M. Grady et al., Geological Society of London, Special publication 140, 153–173, 1998.

Marin, L. E., Field investigations and numerical simulation of groundwater flow in the karstic aquifer of northwestern Yucatan, Mexico, Ph.D. dissertation, Northern Illinois University, Dekalb, Illinois, 183 pp., 1990.

McNeice, G., and A. G. Jones, Multisite, multifrequency tensor decomposition of magnetotelluric data, *Geophysics*, *66*, 158–173, 2001.

Morgan, J., M. Warner, J. Brittan, R. Buffler, A. Camargo, G. Christeson, P. Denton, A. Hildebrand, R. Hobbs, H. Macintyre, G. Mackenzie, P. Maguire, L. Marin, Y. Nakamura, M. Pilkington, V. Sharpton, D. Snyder, G. Suarez, and A. Trejo, Size and morphology of the Chicxulub impact crater, *Nature*, *390*, 472–476, 1997.

Palacky, G. J., Resistivity characteristics of geologic targets, in *Electromagnetic methods in Applied Geophyics*, edited by M. Naibighian, pp. 53–129, Society of Exploration Geophysics, Tulsa, Oklahoma, 1991.

Perry, E., L. Marin, J. McClain, and G. Velazquez, Ring of Cenotes (sinkholes), northwest Yucatan, Mexico: It's hydrogeologic characteristics and possible association with the Chicxulub impact crater, *Geology*, *23*, 17–20, 1995.

Rodi, W., and R. L. Mackie, Nonlinear conjugate gradients algorithm for 2-D magnetotelluric inversion, *Geophysics*, *66*, 174–187, 2001.

Sharpton, V. L., K. Burke, A. Carmargo, S. A. Hall, D. S. Lee, L. E. Marin, G. Suarez-Reynoso, J. M. Quezada-Muñeton, P. D. Spudis, and J. Urrutia-Fucugauchi, Chicxulub Multiring Impact Basin: Size and other characteristics derived from gravity analysis, *Science*, *261*, 1564–1567, 1993.

Ward, W. C., G. Keller, W. Stinnesbeck, and T. Adatte, Yucatan subsurface stratigraphy: Implications and constraints for the Chicxulub Impact, *Geology*, *23*, 873–876, 1995.

M. J. Unsworth, Institute for Geophysical Research, Department of Physics, University of Alberta, Edmonton, Alberta, T6G 2J1, Canada. (unsworth@phys.Ualberta.ca)

O. Campos, Instituto de Geofisica, Universidad Nacional Autonoma de Mexico, Mexico D.F., México.

S. Belmonte, CIIDIR-Oaxaca, Instituto Politecnico Nacional, Hornos 1003, Xoxocotlan 71230, Oaxaca, México. (sbelmont@prodigy.net.mx)

J. Arzate, UNICIT-UNAM, Universidad Nacional Autonoma de Mexico, Campus Juriquilla, Queretaro, México.

P. A. Bedrosian, Department of Earth and Space Sciences, University of Washington, Seattle, WA 98195-1310, USA.